Two New Furanones Isolated from *Coptis deltoidea Rhizome*

Li-Shi Jiang [1,2], Hao-Ran Lei [1], Ze-Feng Niu [2], Yun-Jie Hu[1],

Da-Le Guo [*1] and Yun Deng[*1]

[1] *State Key Laboratory of Southwestern Chinese Medicine Resources, Chengdu University of Traditional Chinese Medicine, Chengdu 611137, People's Republic of China*

[2] *School of Public Health, Chengdu University of Traditional Chinese Medicine, Chengdu 611137, People's Republic of China*

Abstract: Two undescribed furanones (**1**-**2**) were isolated from *Coptis deltoidea* rhizome. HRESIMS, NMR and ECD calculations were used to ascertain their structures. Based on the inflammation cell model of RAW264.7 macrophage which induced by lipopolysaccharides (LPS), RNA-Seq was used to reveal the biological activity of **1**. According to the findings, **1** dramatically changed the genes expression profile of the inflammatory cell model produced by LPS in RAW264.7 cells which indicated that it had potential anti-inflammatory activitiy.

1. Introduction

Rhizoma Coptidis (R*C*) is mainly distributed in Hubei, Sichuan and Chongqing in China [1]. It has many varieties, including the *Coptis chinensis* Franch., *Coptis deltoidea* and *Coptis teeta* Wall. and so on. RC has a very wide range of applications: In clinical, it was the key medicine used to treat diabetes mellitus [2], as well as gastrointestinal diseases [3], skin damage [4] and other diseases. In addition, R*C* was also widely used in food processing and preservation [5]. *C.deltoidea* which belongs to the famous local medicinal herbs of Sichuan [6] has significant development value. Currently, most of the alkaloids were considered as the main active constituents of RC*,* so related studies of RC have focused on the alkaloids include berberine [7], coptisine [8], palmatine [9], epiberberine [10-11], jatrorrhizine [12-13], magnoflorine [14] and other alkaloids. However, with the deepening research of the chemical composition, pharmacological action, processing mechanism and clinical application of RC, more active components particular the non-alkaloid components have attracted more attention [15-16]. At present, the main compounds isolated from RC were main including alkaloids, phenylpropane, flavone, volatile oil and other compounds, such as glycosides, amino acids and organic acids. In this work, two previously undescribed furanones were isolated from *C. deltoidea*. There have been no reports of the isolation of this type compounds from RC yet. The structures were

---

elaborated by thorough analysis of HRESIMS, NMR and ECD calculations. The transcriptomic information of RAW264.7 macrophagesm which treated by the compound **1** screened by RNA-seq technology was analyzed, aiming to reveal the biological activity. The separation and identification process and RNA-Seq results of the obtained compounds were described in detail. The work enriched the diversity of RC's chemical composition and laid a certain material foundation for its further development and utilization.

2. Materials and Methods

2.1. Instruments and Materials

Bruker Ascend 700-MHz and PE One FT-IR spectrometers (Bruker, Massachusetts, USA and PE, Inc., Massachusetts, USA) were used to measure the 1D and 2D NMR and infrared spectrum datas respectively. HRESIMS was performed using a Q Exactive ultrasonic hybrid beam polar orbit mass spectrometer from Thermo Fisher Scientific, Massachusetts, USA. The datas of optical rotation and ultraviolet spectrum were detected by PE Lambda 35 UV-VIS spectrometer (PE, Inc., Massachusetts, USA) and PE Model 241 polarimeter (PE, Inc., Massachusetts, USA). A Chirascan CD spectrometer (APL, Leatherhead, UK) was used to collect circular dichroism spectra. A 250×10.0 mm I.D., 5 μm Ultimate YMC Pack ODS-A column from Japan's YMC was instaled on the NP7000 serials semi-preparative HPLC (Hanbang Sci. & Tech., China) for compounds purification.

2.2. Plant Material

C.deltoidea's roots were provided in July 2020 from Wawushan Pharmaceutical Co., Ltdj in Hongya, Sichuan Province and identified by Chengdu University of TCM professor Ma Yuntong. A voucher specimen (20200716) was deposited in the Laboratory of Traditional Chinese Medicine Chemistry, School of Pharmacy, Chengdu University of TCM.

2.3. Extraction and Isolation

Ten kilograms of powdered *C. deltoidea* roots was extracted by percolation with 70% methanol solution. After concentrated by rotating in a vacuum, the extract (2.6 kg) was dispersed and dissolved with hot water and extracted by PE, EtOAc and n-buOH successively to afford PE (12 g), EtOAc (102.0 g), n-buOH (1000.0 g), and H_2O (1000.0 g) soluble fractions.

Using the macro-porous resin D101, which eluted gradually with MeOH-H_2O ratios of 70:30, 80:20, 90:10 and 95:5, the PE component (12g) was divided into four parts (PD101-1~4). Then the EtOAc extract (102g) was frationated by a macro-porous resin D101 [a gradient of MeOH-H_2O was used for eluting (30:70, 40:60, 50:50, 60:40, 70:30, 80:20, 90:10, and 95:5)] and separated into nine fractions (ED101-1~9). The fourth part of PE (PD101-4) and the ninth EtOAc part (ED101-9) was put together (30g) under the guidance of TLC analysis and subjected to a C_{18} medium pressure column using MeOH-H_2O (35:65) as eluents to obtain 11 fractions (F1-F13). F1 (3.5g) was isolated over a Sephadex LH-20 gel column and chloroform-MeOH (50:50) was used as eluent to afford 7 sub-fractions (F1.1-F1.7). The sub-fraction F1.4 (0.2g) was further purified and prepared by semi-preparative HPLC under UV detection (210 nm, 254 nm) with MeOH-H_2O (60:40, 3 mL/min) for the preparation of **1** (1 mg, t_R =19 min). Fraction ED101-2 (20.0 g) was subjected three sections (Fr1-3) after passing through Sephadex LH-20 column [chloroform-MeOH (50:50) as eluent. Subfraction Fr4 (7g) was subjected to a silicagel column to collected fifteen subfractions (Fr4.1-Fr4.15) under the condition of petroleum ether-acetone (100:1~0:1) acting as an elution. Subfraction Fr4.2 (0.1g) had been purified by using semi-preparative HPLC under UV detection (210 nm, 254 nm) with MeOH-H_2O (50:50~100:0, 3 mL/min, 30min) to prepare **2** (1 mg, t_R = 21 min).

Compound **1**: white powder; $[\alpha]_D^{25}$ = +22.0 (c 0.037, MeOH); λ_{max} = 196 (1.58) in the UV (MeOH); IR (KBr) ν_{max}: 3422, 2962, 2925, 2854, 1641, 1261, 1096 cm^{-1}; HRESIMS *m/z* 261.0757 [M+H]$^+$ (computed for $C_{14}H_{14}O_5^+$, 261.0758). ^{1}H NMR and ^{13}C NMR datas were showed on Table 1 and 2.

Compound **2**: white amorphous powder; $[\alpha]_D^{25}$= +17.3 (c 0.034, MeOH); λ_{max} = 196 (1.58) in the UV (MeOH); IR (KBr) v_{max}: 2924, 2849, 1770, 1486, 1279, 1091 cm^{-1}; HRESIMS *m/z* 273.0758 [M+H]$^+$ (computed for $C_{15}H_{13}O_5^+$, 273.0758); ^{1}H NMR and ^{13}C NMR data were showed on Table 1 and 2 .

2.4. ECD Calculations

The primary tool used for the theoretical calculations on **1** and **2** was Gaussian 16 (Gaussian Inc., CT). First of all, Conflex 8 was used to conduct a conformational analysis with a search limit of 5 Kcal/mol [17]. Second, DFT was used to optimize possible conformers (Boltzmann distribution>1%) with the B3LYP/6-31G (d, p) layer in gas and subsequently at B97XD/DGDZVP in methyl alcohol [18]. Each geometrical conformer's Boltzmann dispersion rate was measured to complete the ECD spectrum. The Gauss curve (0.3 eV) which was obtained after Boltzmann statistical weighting and summing the individual CD spectra using SpecDis 1.71 was compared with experimental data [19-20].

2.5. RNA-Seq

Raw 264.7 macrophages (a density of 1×10^6) were inoculated in tissue culture plate 6. When the concentration of cultured cells reached 60%‑70%, three groups were formed: the medication administration group, the DMSO group and the LPS group[21]. DMSO group was treated with DMSO for 24 hours, LPS (1µg/mL) was used to stimulate the LPS group for 24 hours, and drug administration group was stimulated with LPS (1µg/mL) for 24 hours after treatmented with **1** for 2 hours at a concentration of 60 µM. Following the collection of the three cell groups, RNA Isolater Total RNA Extraction Reagent (Vazyme) was used for obtaining RNA from cells, then AGE was used to measure the concentration and purity of the collected RNA. Next-Generation Sequencing (NGS) based on the Illumina sequencing platform was used to test double-end sequencing. Using the FastQC tool, raw data quality control was carried out. HISAT2 program was used to compare each clean read separately to the reference genome. Differentially expressed genes (DEGs) were assessed using the DESeq 2R program. Significantly differentially expressed genes (DEGs) were defined as those with a FoldChange 1.2 and a p-correction value 0.05. The clusterProfiler R package was used to visualize data using R software, including heat maps, volcano plots, KEGG plots and GSEA plots[22].

3. Results and Discussion

3.1. Structure Elucidation

White powder was identified as Compound **1**. The pseudo-molecular ion peak in HRESIMS determined its molecular formula to be $C_{14}H_{12}O_5$. From ^{1}H-NMR spectrum of **1** (Table 1) , four aromatic protons at δ 8.74-8.72 (1H, m, H-4), 7.52 (1H, d, *J*= 9.1 Hz, H-5), 8.5-8.48 (1H, m, H-9), 7.57 (1H, d, *J* = 8.6 Hz, H-10); two oxygenated methyl at δ 4.02 (3H, s, 7-OCH$_3$), 4.04 (3H, s, 6-OCH$_3$) and one methines at δ 6.35 (1H, s, H-12) could be inferred. In the ^{13}C NMR spectra of **1**, ester carbons were among the 14 carbon signals at δ 169.2 (C-1); ten aromatic carbons at δ144.4 (C-11), 119.6 (C-10), 129.6 (C-9), 130.4 (C-8), 143.5 (C-7), 150.1 (C-6), 117.8 (C-5), 120.5 (C-4), 124.3 (C-3), 122.1 (C-2); two oxygenated methyl at δ 61.6 (C-7-OCH3), 56.8 (C-6-OCH3) and one methine at δ102.4 (C-12). The ^{1}H-^{1}H COSY relevance of H-9 /H-10, H-5 /H-4 showed the presence of a naphthalene moiety. HMBC relevance of OCH$_3$/C-7, OCH$_3$/C-6 showed the two oxygenated methyl was identified at the C-6 and C-7 positions. A carbonylated tetrahydrofuran structure was speculated combined the signals of ester carbons at δ 169.2 (C-1) and methine at δ 102.4 (C-12). The structure of the five-membered rings was decided by related signals of HMBC relevance of H-12/C-2, C-1. As the computed ECD curve of *R*-12 matched the experiment spectra neatly (Figure 3A), the definitive confirmation of **1**'s absolute configuration was depicted in Figure 1.

White powder was identified as compound 2. From pseudo-molecular ion peak in HRESIMS, its molecular formula was assigned as $C_{15}H_{14}O_5$ .The ^{1}H and ^{13}C NMR datas of **2** were ery similar to **1**

except the added signal of a oxygenated methyl （δ 3.64, 3H, s, 12-OCH$_3$). From the ^{1}H-NMR spectrum of **2** (Table 1) , four aromatic protons at δ 8.75-8.71 (1H, m,H-4), 7.52 (1H, d, J= 9.1 Hz,H-5), 8.51-8.47 (1H,m,H-9), 7.57 (1H, d, J=8.6Hz, H-10); three oxygenated methyl at δ 4.02 (3H, s, 7-OCH$_3$), 4.04 (3H, s, 6-OCH$_3$) , 3.64 (3H, s,12-OCH$_3)$ and one methine at 6.35 (1H, s,H-12) could be visible in the ^{13}C NMR spectra of compound 2. There were 15 carbons cluding one ester carbon at δ169.2 (C-1) ; ten aromatic methines carbons at δ 144.4 (C-11), 119.6 (C-10), 129.6 (C-9), 130.5 (C-8), 143.6 (C-7), 150.1 (C-6), 117.9 (C-5), 120.5 (C-4), 124.3 (C-3), 122.1 (C-2); three oxygenated methyl at δ 61.6 (C-7-OCH3), 56.8 (C-6-OCH3), 56.7 (C-12-OCH$_3$) and one methine at δ 102.4 (C-12). The HMBC correlations of 3.64 (3H, s) /C-12, 4.04 (3H, s)/C-6, 4.02 (3H, s)/C-7 showed the oxygenated methyl was connected C-12, C-6 and C-7. The position of the methoxy group at C-6, C-7 were confirmed by the relevance of H-9 /H-10, H-5 /H-4 on ^{1}H-^{1}H COSY. As the calculated ECD curve of 12-R match the experimental spectrum neatly (Figure 3B), the definitive confirmation of **2**'s absolute configuration was depicted in Figure 1.

	R
1	OH
2	OCH$_3$
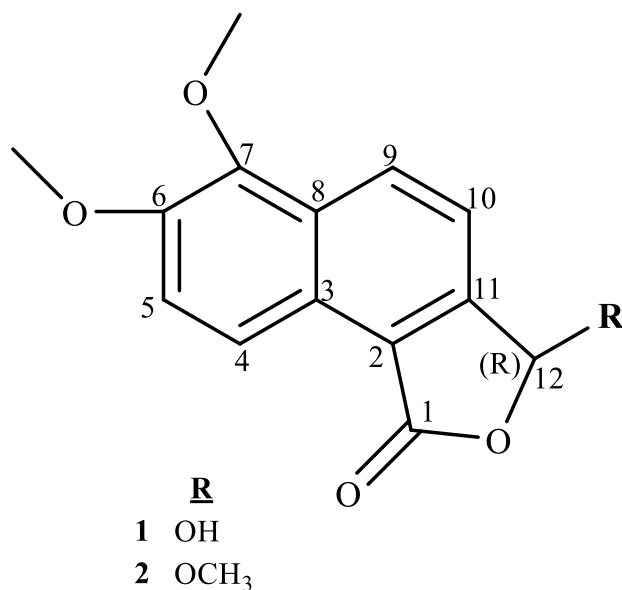
Figure 1. Chemical structures of **1** and **2**

	R
1	H
2	CH$_3$
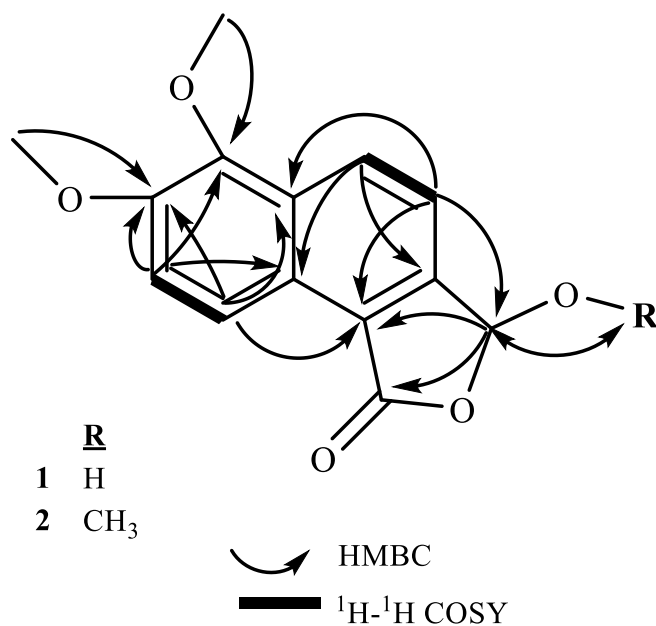
HMBC

^{1}H-^{1}H COSY

Figure 2. Key HMBC (arrows) and ^{1}H-^{1}H COSY (bold) correlations of **1** and **2**

Table 1. ^{1}H (700 MHz) and ^{13}C (175 MHz) NMR spectroscopic datas for **1** and **2** (Chloroform-d)

Position	1				2			
	δC	δH	COSY*	HMBC	δC	δH	COSY*	HMBC
1	169.2				169.2			
2	122.1				122.1			
3	124.3				124.3			
4	120.5	8.74-8.72 (1H, m)	5	2,8,7,6	120.5	8.75 -8.71 (1H, m)	5	2,8,7,6
5	117.8	7.52 (1H, d, 9.1)	4	3,7,6	117.9	7.52 (1H, d,9.1)	4	3,7,6
6	150.1				150.1			
7	143.5				143.6			
8	130.4				130.5			
9	129.6	8.5-8.48 (1H, m)	10	3,11	129.6	8.51 -8.47 (1H, m)	10	3,11
10	119.6	7.57 (1H, d,8.6)	9	12,2,8	119.6	7.57 (1H, d,8.6)	9	12,2,8
11	144.4				144.4			
12	102.4	6.35 (1H, s)		2,1	102.4	6.35 (1H, s)		2,1,12-OCH$_3$
6-OCH$_3$	56.8	4.04 (3H, s)		6	56.8	4.04 (3H, s)		6
7-OCH$_3$	61.6	4.02 (3H, s)		7	61.6	4.02 (3H, s)		7
12-OCH$_3$					56.7	3.64 (3H, s)		12

*^{1}H-^{1}H
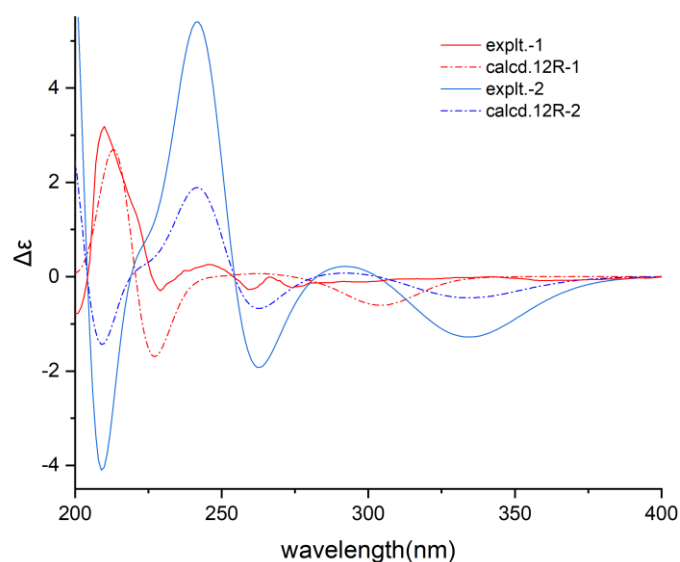
Figure 3. Calculated ECD spectra and experimental ECD curves of **1** and **2**

3.2. RNA-Seq Analysis
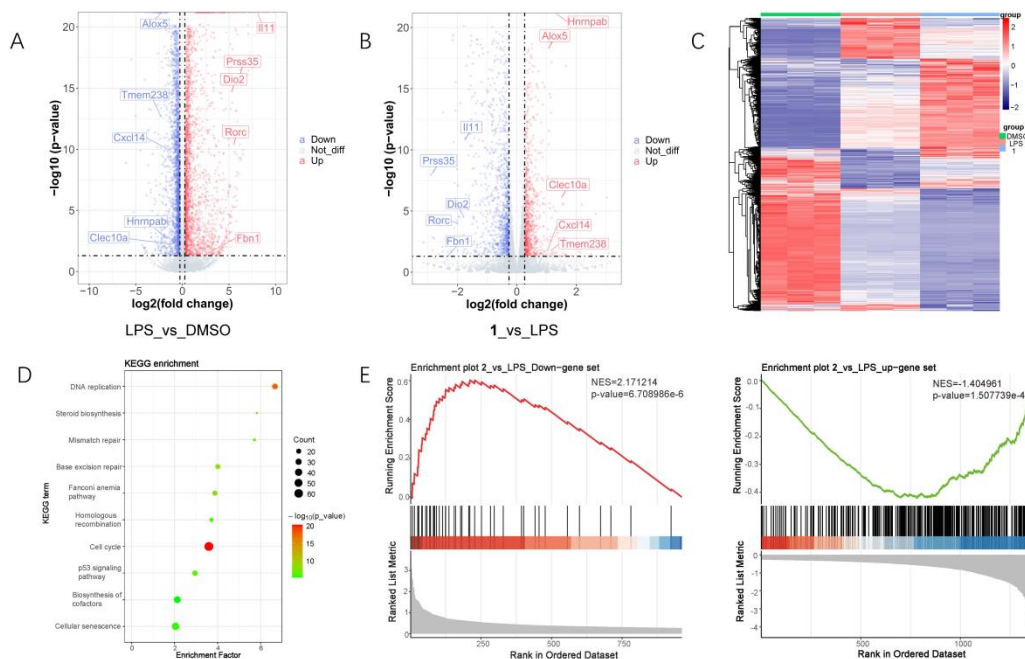
Figure 4. Reversed LPS-induced inflammatory phenotypic gene expression in RAW264.7 cells

(A) A volcano plot of DEGs in RAW264.7 macrophages treated with LPS versus DMSO was shown; red dots indicate DEGs obviously upregulated by LPS vs DMSO, blue dots indicate significantly downregulated DEGs. (B) A volcano plot of DEGs in RAW264.7 macrophages treated with LPS + **1** compared to LPS; red dots indicate DEGs obviously upregulated by LPS vs DMSO and blue dots indicate significantly downregulated DEGs. (C) Heat map of DEGs in DMSO, LPS and LPS +**1** treated RAW264.7 macrophages. (D) DEGs' KEGG enrichment analysis. (E) Analysis of GSEA enrichment.

3.2.1 Transcriptome Analysis of Compound **1**

Three groups of RAW264.7 cells were established, DMSO control group (treated with DMSO), LPS induction group (treated with LPS+DMSO) and drug administration group (treated with LPS and **1**). To illustrate **1**'s biological activity, RNA of different group cells were extracted for transcriptome analysis. Variable genes were identified by RNA-seq conditional screening (FoldChange>1.2, p<0.05) and visualized by plotting volcanoes separately (Figure 4A and 4B). In comparison to the DMSO group, the LPS group showed up-regulation of 3737 genes and down-regulation of 4035 genes. Comparison to the LPS group, the LPS+**1** group showed up-regulation of 1213 genes and down-regulation of 962 genes. During the screening of differential genes we found many genes were worthy of attention. For example, Ccl14 acted as a chemokine that promoted inflammatory cell activation [23] and was downregulated after drug administration; Il11 has pro-inflammatory effects and was downregulated after drug administration [24]. A heat map (Figure 4C) showed the expression of the 2175 differential genes obtained by comparing the administered group with the LPS-induced group between the three groups (Figure 4C) revealing that the administration of the drug reversed some of the LPS-induced gene expression. In addition, KEGG enrichment analysis was performed using the DEG of the LPS group versus the drug administration group, and the 10 most significantly enriched pathways were obtained by conditional screening (FoldChange>1.2, *p*<0.05) (Figure 4D). GSEA enrichment analysis showed that **1** was positively correlated with the down-regulated genes set of LPS treatment after intervention. Conversely, following intervention, the up-regulated genes set of LPS

treatment showed a negative connection with **1** (Figure 4E). Taken together, compound **1** dramatically altered the RAW264.7 cells' LPS-induced inflammatory cell model's gene expression profile.

Acknowledgments

Supporting Information

Supporting information accompanies this paper on http://www.acgpubs.org/journal/records-of-natural-products

ORCID
Li-Shi Jiang: 0000-0002-2223-7979
Hao-Ran lei: 0009-0009-4107-5969
Ze-Feng Niu: 0009-0006-9430-0048
Yun-Jie Hu: 0000-0001-7282-6993
Da-Le Guo: 0000-0003-3219-7066
Yun Deng: 0000-0002-3428-8992

References

[1]   S. R. Cao, H. Du, B. B. Tang, C. X. Xi and Z. Q. Chen (2021). Non-target metabolomics based on high-resolution mass spectrometry combined with chemometric analysis for discriminating geographical origins of *Rhizoma coptidis*, *Microchem. J.* **160**, 105685.

[2]   W. R. An, Y. Q. Huang, S. Q. Chen, T. Teng, Y. N. Shi, Z. H. Sun and Y. S. Xu (2021). Mechanisms of *Rhizoma Coptidis* against type 2 diabetes mellitus explored by network pharmacology combined with molecular docking and experimental validation, *Sci. Rep.* **11**, 20849.

[3]   Z. Zhong (2022). Current advances in C*optidis rhizoma* for gastrointestinal and other cancers, *Front. Pharmacol.* **12**, 775084.

[4]   S. Q. Wu, D. Q. Yu, W. Y. Liu, J. Zhang, X. J. Liu, J. K. Wang, M. Yu, Z. X. Li, Q. F. Chen, X. G. Li and X. L. Ye (2020). Magnoflorine from *Coptis* chinese has the potential to treat DNCB-induced Atopic dermatits by inhibiting apoptosis of keratinocyte, *Bioorg. Med. Chem.* **28**, 115093.

[5]   L. S. Jiang, X. F. Zuo, X. M. Zhang, Y. Luo, X. A. Li ,W. X. Guo and Y. Deng (2022). Bacteriostasis of *Coptis* on intestinal pathogens in vitro, *Food Ferment. Ind.* **48**, 101-105．

[6]   L. Y. Ni, T. Z. Chen and Q. M. Fang (2021). Evolution of Sichuan Dao-di herbs recorded in ancient works of materia medica of different historical periods, *China J. Chin. Mater. Med.* **46**, 1564-1573.

[7]   G. Chandirasegaran, C. Elanchezhiyan, K. Ghosh and S. Sethupathy (2017). Berberine chloride ameliorates oxidative stress, inflammation and apoptosis in the pancreas of Streptozotocin induced diabetic rats, *Biomed. Pharmacother.* **95**, 175-185.

[8]   F. N. Chai, W. Y. Ma, J. Zhang, H. S. Xu, Y. F. Li, Q. D. Zhou, X. G. Li and X. L. Ye (2018). Coptisine from *Rhizoma Coptidis* exerts an anti-cancer effect on hepatocellular carcinoma by up-regulating miR-122, *Biomed. Pharmacother.* **103**, 1002-1011.

[9]   J. S. Wu, W. G. Huang, Y. Luo, Y. Hou, P. Wang and X. L. Meng (2018). Study on the underlying mechanism of regulating effect on NLRP3 inflammasome pathway of palmatine chlorid ，an isoquinoline alkaloid from *Coptidis rhizoma*, *Clin. Pharmacol. Ther.* **34**, 26-29.

[10]   L. Liu, J. Li and Y. He (2020). Multifunctional epiberberine mediates multi-therapeutic effects, *Fitoterapia* **147**, 104771.

[11]   Y. Xiao, J. Deng, C. Li, X. Gong and X. Li (2021). Epiberberine ameliorated diabetic nephropathy by inactivating the angiotensinogen (Agt) to repress TGFβ/Smad2 pathway, *Phytomedicine.* **83**, 153488.

[12]   F. R. Zhong, Y. Chen, J. Chen, H. L. Liao, Y. R. Li and Y. T. Ma (2021). Jatrorrhizine: A review of sources, pharmacology, pharmacokinetics and toxicity, *Front. Pharmacol.* **12**, 783127.

[13] Y. Zhou, Y. H. Wang, C. T. Vong, Y. Y. Zhu, B. J. Xu, C. C. Ruan, Y. T. Wang and W. S. Cheang (2022). Jatrorrhizine improves endothelial function in diabetes and obesity through suppression of endoplasmic reticulum stress, *Int. J. Mol. Sci.* **23**, 12064.

[14] Y. Shen, X. Fan, Y. Qu, M. Tang, Y. Huang, Y. Peng and Q. Fu (2022). Magnoflorine attenuates inflammatory responses in RA by regulating the PI3K/Akt/NF-κB and Keap1-Nrf2/HO-1 signalling pathways in vivo and in vitro, *Phytomedicine* **104**, 154339.

[15] L. L. Shi, W. H. Jia, L. Zhang, C. Y. Xu and G. H. Du (2019). Glucose consumption assay discovers coptisine with beneficial effect on diabetic mice, *Eur. J. Pharmacol.* **859**, 172523.

[16] M. Qu, Y. Wang, S. Cao, Y. Liu, D. Liu, F. Qiu and N. Kang (2020). Main alkaloids of *Rhizoma Coptidis* improved palmitic acidinduced insulin resistance in HepG2 cells via AMPK and MAPK signaling pathway, *Asian J. Tradit. Med.* **15**, 239-254.

[17] Y. M. Cao, D. L. Guo, M. Y. Jin, L. Tan, T. L. Yang, F. Deng, Y. C. Gu, X. H. Li, Z. X. Cao and Y. Deng (2021). Two new nor-sesquiterpenoids from *Fusarium tricinctum*, an *endophytic fungus* isolated from *Ligusticum chuanxiong*, *Nat. Prod. Res.* **35**, 3535-3539.

[18] D. L. Guo, L. Qiu, D. Feng, X. He, X. H. Li, Z. X. Cao, Y. C. Gu, L. Mei, F. Deng and Y. Deng (2020). Three new α-pyrone derivatives induced by chemical epigenetic manipulation of *Penicillium herquei*, an *endophytic fungus* isolated from *Cordyceps sinensis*, *Nat. Prod. Res.* **34**, 958-964.

[19] F. Ju, Q. X. Kuang, Q. Z. Li, L. J. Huang, W. X. Guo, L. Q. Gong, Y. F. Dai, L. Wang, Y. C. Gu, D. Wang, Y. Deng and D. L. Guo (2021). Aureonitol analogues and orsellinic acid esters isolated from *chaetomium elatum* and their antineuro inflammatory activity, *J. Nat. Prod.* **84**, 3044-3054.

[20] J. Yan, W. X. Guo, L. Y. Zhou, Z. X. Cao, J. Pei, Y. Deng, B. Li, D. Liu, D. L. Guo and C. Peng (2022). A Neoprzewaquinone Analogue from *Salvia miltiorrhiza Bunge*, *Rec. Nat. Prod.* **16**, 572-578.

[21] Q. X. Kuang, Y. Luo, L. R. Lei, W. X. Guo, X. A. Li, Y. M. Wang, X. Y. Huo, M. D. Liu, Q. Zhang, D. Feng, L. J. Huang, D. Wang, Y. C. Gu, Y. Deng and D. L. Guo (2022). Hydroanthraquinones from *nigrospora sphaerica* and their antiinflammatory activity uncovered by transcriptome analysis, *J. Nat. Prod.* **85**, 1474-1485.

[22] S. N. Li, X. A. Li, Q. Zhang, Y. J. Hu, H. R. Lei, D. L. Guo, L. S. Jiang and Y. Deng (2023). Chemical constitutes from *Tuber indicum* with immunosuppressive activity uncovered by transcriptome analysis, *Fitoterapia* **173**, 105773.

[23] Y. Gu, X. Li, Y. Bi, Y. Zheng and Y. Huang (2020). CCL14 is a prognostic biomarker and correlates with immune infiltrates in hepatocellular carcinoma, *Aging* **12**, 784-807.

[24] A. A. Widjaja, S. Chothani, S. Viswanathan, J. W. T. Goh, W. W. Lim and S. A. Cook (2022). IL11 stimulates IL33 expression and proinflammatory fibroblast activation across tissues, *Int. J. Mol. Sci.* **23**, 8900.